Bulletin of the Geological Society of Malaysia, Volume 81, May 2026, pp. 31 - 41
DOI: https://doi.org/10.7186/bgsm81202604

Physico-chemical condition and origin of Au mineralisation at Me Xi deposit, Central Truong Son Belt, Vietnam: Insight from fluid inclusion studies

Truong Xuan Le[1,2,3,*], Khin Zaw[4], Hai Thanh Tran[1], Khang Quang Luong[1,3], Du Khac Nguyen[1,2,3], Ban Xuan To[1]

[1] Faculty of Geosciences and Geoengineering / Economic Geology and Sustainable Development Research Team (EGSD), Hanoi University of Mining and Geology, Hanoi, Vietnam
[2] Centre for Excellence in Analysis and Experiment, Hanoi University of Mining and Geology, Hanoi, Vietnam
[3] Economic Geology and Sustainable Development Research Team (EGSD), Hanoi University of Mining and Geology, Hanoi, Vietnam
[4] CODES Centre Ore Deposit and Earth Sciences, University of Tasmania, Private Bag 126, Hobart, Tasmania 7001, Australia
* Corresponding author email address: lexuantruong@humg.edu.vn

Abstract: The Me Xi gold deposit is an underexplored hydrothermal gold system in the central Truong Son Belt, Vietnam. This study investigates the physico-chemical condition and origin of the ore-bearing fluids at Me Xi based on fluid inclusion analyses. Only primary fluid inclusions are studied, and they are two-phase (i.e., vapor and liquid) inclusions and predominantly less than 10 μm in size, with liquid occupying approximately 70-90% of the inclusion volume. They display homogenization temperatures ranging from 181°C to 394°C (n=77), with a dominant population clustering between 180°C and 260°C (n=56). Fluid salinities range from 0.3 to 16.9 wt.% NaCl (n=57) with the majority comprising moderate to high-salinity inclusions (5-17 wt.%; n=47), which suggests a significant magmatic contribution. The subordinate low-salinity inclusions (<5 wt.%; n=10) are possibly indicative of locally diluted hydrothermal fluids caused by meteoric water and fluid-carbonaceous host rocks interaction. The combined thermometric and salinity data support an isothermal mixing model between magmatic and meteoric fluids, which appears to be a key mechanism for gold precipitation. The magmatic-sourced fluids in the deposit are spatially associated with the nearby dolerite intrusions.

Keywords: Me Xi, Quang Tri, Truong Son Belt, Au mineralisation, fluid inclusion, economic geology, Vietnam

INTRODUCTION

The Truong Son Belt (TSB) is a significant geological domain within the Indochina Block. Its northern boundary is marked by the Song Ma Suture Zone, and its southern boundary is defined by the Tam Ky-Phuoc Son Suture Zone (TPSZ) (Figure 1a). The geological history of the TSB is predominantly influenced by the Ordovician-Silurian (O-S) Caledonian and Permian-Early Triassic (P-T_1) Indosinian orogenies (e.g., Dung *et al.*, 2024).

The TSB is a highly prospective metallogenic belt within the Indochina Block, particularly for gold (Au), copper (Cu), and lead-zinc (Pb-Zn) mineralisation (Khin Zaw *et al*., 2014). These deposits occur in various mineralisation styles throughout the region and are primarily hosted in Cambrian to Devonian sedimentary sequences that have been mainly metamorphosed to greenschist facies (Lepvrier *et al*., 2004; Khin Zaw *et al*., 2014). The most prospective metallogenic region within the TSB and its adjacent geological structures is considered to be the TPSZ where various mineralisation styles and deposits have been discovered. These include the Bong Mieu skarn and sediment-hosted/orogenic Au (±W) systems and the Duc Bo Cu-Zn-Pb volcanic-hosted massive sulphide (VHMS) deposit in Vietnam (Khin Zaw *et al*., 2014); the Phuoc Son intrusion-related Au-Pb-Zn deposit (Manaka, 2014); and the Sepon Cu-Au porphyry-skarn and Carlin-like Au deposits in Laos (Cromie, 2010). In the northern part of the TSB in Laos, the Phu Kham epithermal Au (Khin Zaw *et al*., 2014) and low-sulfidation epithermal Au deposits at Phu He and Ban Houayxai (Manaka, 2008) have been reported.

In the central TSB in Vietnam (i.e., Quang Binh and Quang Tri provinces), approximately 30 gold prospects have been identified. In Quang Tri province, in addition to the Me Xi deposit, there are numerous similar types of deposits distributed throughout the region. Meanwhile, in Quang Binh province, notable prospects include Khe Nang

0126-6187; 2637-109X / Published by the Geological Society of Malaysia.

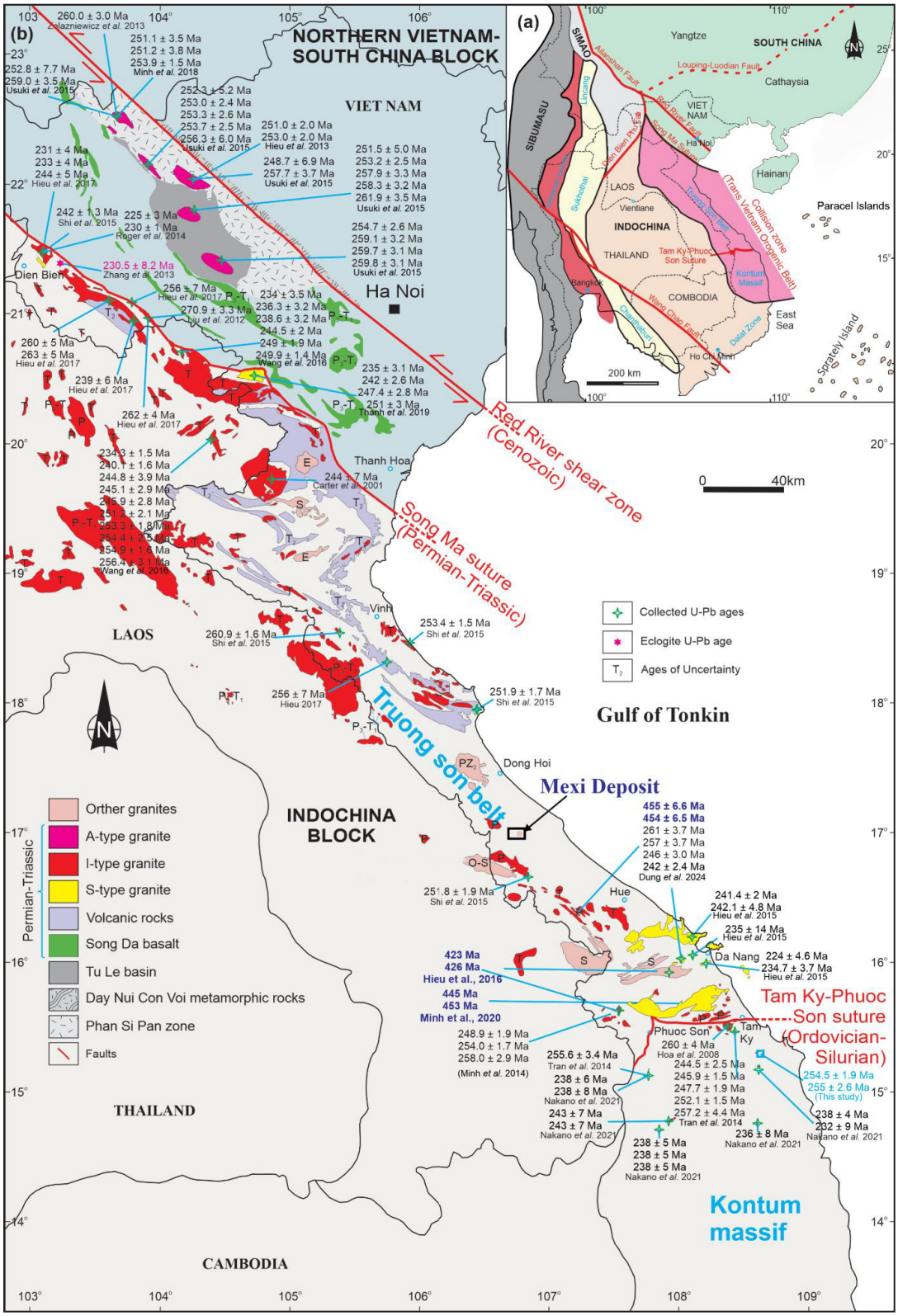

Figure 1: (a) The tectonic setting of the Me Xi Au deposit in the Indochina Block (modified from Dung *et al*., 2024; Le *et al*., 2026); (b) Simplified geological map of the Indochina block showing O-S and P-T magmatism (geochronological data sources: Carter *et al*., 2001; Hoa *et al*., 2008; Liu *et al*., 2012; Żelaźniewicz *et al*., 2013; Hieu *et al*., 2013, 2015, 2017; Zhang *et al*., 2013; Tran *et al*., 2014; Roger *et al*., 2014; Shi *et al*., 2015; Wang *et al*., 2016; Minh *et al*., 2018; Thanh *et al*., 2019; Hung *et al*., 2022 and Dung *et al*., 2024). Note: in Vietnamese, Paracel Islands = Hoang Sa and Spratly Islands = Truong Sa.

- Khe Net, Khe Dap - Khe Truong - Khe Da Trang, Suoi Kin, Xa Khia, Khe Reu, Bach Dan, Duong 10, Duong 16, Lang Ho, Thu Lu, and Dong Vang. These hydrothermal gold mineralisation systems are primarily hosted in by sedimentary rocks which have been metamorphosed at greenschist to amphibolite facies (Lepvrier *et al*., 2004) and most of them remain underexplored and poorly understood.

The Me Xi Au deposit in Quang Tri province has been initially studied to investigate the Au mineralisation style of the central TSB. Le *et al.* (2015) presented pyrite morphologies and geochemistry from various hydrothermal stages at the deposit, confirming that they are different from the nearby Sepon Au-Carlin-like system. Le *et al*. (2024) recently studied the basic mineralisation characteristics of the deposit based on field mapping, core logging, and petrographic analyses of the lithologies and mineralisation zones. This study aims to examine the physico-chemical conditions and sources of ore-bearing fluids in the Me Xi deposit, central TSB based on fluid inclusion analyses.

GEOLOGICAL SETTING AND AU MINERALISATION

Geological setting

Regional geology

The regional geology of the TSB is shown in Figure 1b. The magmatic and tectonic evolution of the region is predominantly influenced by two major events: the Ordovician-Silurian (O-S) Caledonian and the Permian-Early Triassic (P-T1) Indosinian orogenies.

The Caledonian orogeny commenced with bilateral subduction between the TSB and the Kon Tum Massif (KTM) during ~520-450 Ma, followed by a subsequent collision during ~450-430 Ma along the TPSZ (Dung *et al*., 2024). Magmatic activity in this event includes sporadic pre-collisional I-type granites (~452 Ma) located north of the TPSZ (Dung *et al*., 2024), along with diorite (~470 Ma) and rhyolitic tuff (~476 Ma) recorded in southeastern Laos (Gardner *et al*., 2017). In the KTM, extensive magmatic activity is recorded, characterized by mafic to felsic rocks (~476-488 Ma and ~457-467 Ma) west of the Poko Fault and diorite to granite (451-457 Ma, 468 Ma, 473-485 Ma) in areas south of the TPSZ and east of the Poko Fault (Thuy *et al*., 2024; Hieu *et al*., 2015; Trong *et al*., 2021; Nagy *et al*., 2001). The collision between the KTM and TSB is evidenced by syn-collisional intrusive rocks (~455-445 Ma) of the Chu Lai Complex located north of the TPSZ (Jiang *et al*., 2020; Minh *et al*., 2020) and by S-type granites (~428 Ma) of the Song Chay Complex in northeastern Vietnam (Roger *et al*., 2000). This collision triggered widespread greenschist-facies metamorphism, accompanied by local zones of higher-grade metamorphic rocks (Tran Van Tri *et al*., 2009). Post-collisional magmatism is represented by intermediate to granitic rocks of the Dai Loc Complex (~415-423 Ma) north of the TPSZ (Jiang *et al*., 2020; Trong *et al*., 2021), along with scattered O-S igneous rocks mapped south of the TSB (Duong *et al*., 1996).

The Indosinian orogeny began with subduction between the South China and Indochina Blocks during the Early Permian, culminating in a collision during the Early Triassic along the Song Ma Suture Zone (Dung *et al*., 2024). Evidence for the subduction phase includes intermediate to I-type granitic intrusions (~290–245 Ma) throughout the TSB and KTM, including ~260 Ma rocks of the Dien Bien Complex along the Song Ma Suture Zone and central TSB (Shi *et al*., 2015; Hieu *et al*., 2017). During the collision phase, S-type granites (~245–230 Ma) were emplaced (Hieu *et al*., 2015), in conjunction with the formation of metamorphic rocks ranging from greenschist- to amphibolite-facies within the TSB (Carter *et al*., 2001; Lepvrier *et al*., 2004) and amphibolite to granulite facies metamorphism in the KTM (Maluski *et al*., 2005).

Local geology

The sedimentary rocks in the Me Xi area are composed of two main units, siltstone-sandstone and siltstone-shale of the Long Dai Formation, which has been mapped as Ordovician-Early Silurian in age. The siltstone-sandstone unit comprises thinly-bedded siltstone interbedded with thin or lens-shaped sandstone (Le *et al*., 2024; Figure 2). The siltstone-shale unit consists of siltstone and calcareous siltstone alternating with shale, black shale, and calcareous shale (Le *et al*., 2024).

Magmatic rocks in the area include undated porphyritic dolerite and mafic dykes of which the dolerite has been recently dated as ~430 Ma (Le *et al*., 2026). The porphyritic dolerite located approximately 3 km southwest of the Me Xi deposit centre. This rock type contains ~40% dark minerals, including olivine, pyroxene, biotite and hornblende, and ~60% plagioclase (Le *et al*., 2024). The rock exhibits intense hydrothermal alteration, with common secondary minerals such as chlorite, epidote, and sericite (Le *et al*., 2024). Mafic dykes are characterized by fine-grained textures and a greyish-green hue. They are observed in both drill cores and outcrops near the deposit (Le *et al*., 2024). Both rock types contain narrow quartz-sulphide veins hosting pyrite, pyrrhotite, sphalerite, galena, and chalcopyrite, along with associated alteration minerals (Le *et al*., 2024).

Au mineralisation in the Me Xi deposit

The Me Xi deposit consists of eight Au-bearing mineralized bodies distributed across two zones (Figure 2). The main mineralised zone extends approximately 640 m in length and ranges from 10 to 60 m in width. It hosts the most significant Au-bearing bodies, including a high-grade interval of 3m@51.7 g/t Au (Axiom, 2006). The second zone, located southwest of the main zone, contains two smaller Au-bearing bodies with a combined length of ~160 m and an average thickness of 0.5-2 m (Le *et al*., 2024).

Au mineralisation is hosted within hydrothermal quartz-sulphide stockwork veins cross cutting the metasedimentary rocks of the Long Dai Formation. Four distinct stages of

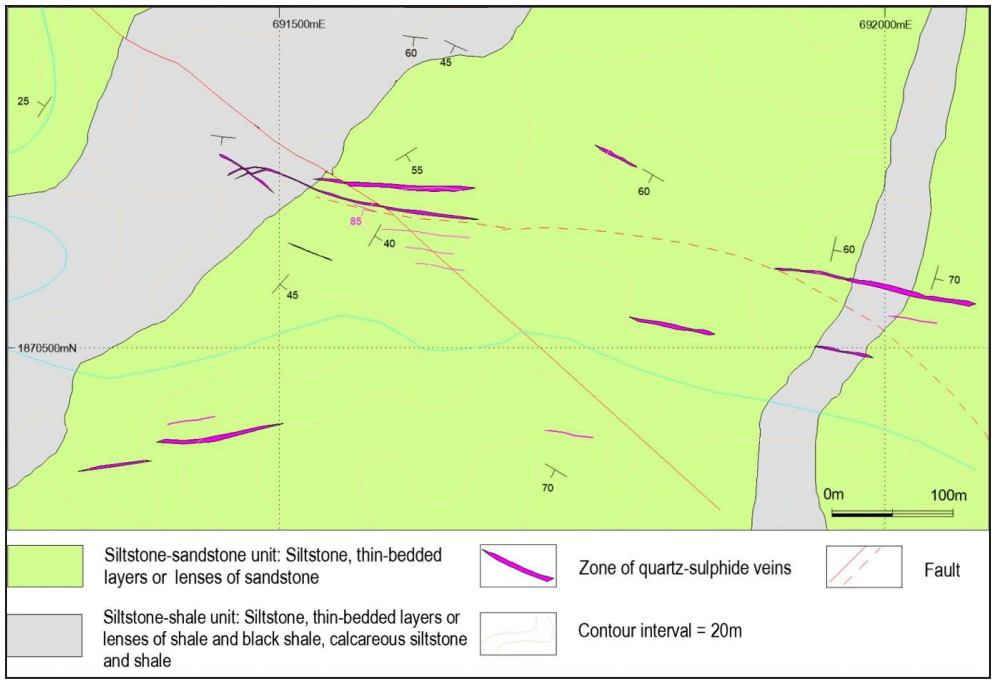

Figure 2: Geological map of the Me Xi Au deposit (Le *et al*., 2024).

mineralisation have been identified by Le *et al*. (2024), including: pre-Au Stage 1 (Quartz - pyrite – chalcopyrite); Syn-Au Stage 2 (Quartz - chlorite - calcite - pyrite - pyrrhotite - arsenopyrite - galena - chalcopyrite - gold); Syn-Au Stage 3 (Quartz - sericite - chlorite - calcite - pyrite - chalcopyrite - galena – gold); and post-Au Stage 4 (Quartz - calcite - pyrite – chalcopyrite).

SAMPLE COLLECTION

Eight samples of quartz from Au-bearing hydrothermal vein stage were selected for fluid inclusion studies (Figure 3). All mineralised zones have stockwork textures, in which quartz-sulphide veins are commonly less than 2-3 cm thick. Quartz associated with sulphides in the Au-bearing intervals was prioritized for fluid inclusion analysis. Thin sections of hand specimens were examined under a microscope to identify quartz crystals containing sufficient fluid inclusions. Selected samples were then prepared as double-polished thin sections for detailed fluid inclusion studies.

METHODOLOGY

The analyses were conducted at the Centre for Ore Deposit and Earth Sciences (CODES), University of Tasmania, Australia. A brief overview of the analytical techniques and thermal parameter measurements is provided below, while detailed descriptions of the methodology are available in Roedder (1984) and Wilkinson (2001).

The fluid inclusion sections were initially investigated under a ZEISS polarizing microscope for their textural features, including the sizes and phases of fluid inclusions. Primary inclusions are commonly observed in the crystal growth zone or as isolated occurrences, while secondary inclusions usually exhibit planar and linear distribution with smaller size. Secondary inclusions were excluded from this study. The sections were soaked in acetone for at least 24 hours to detach the sample from the glass base and were then cut into chips containing areas of primary inclusions (approximately <1 cm in diameter). These chips were analysed using a THMSG600 heating-freezing stage (Linkam, UK) to determine the initial and last melting temperatures and homogenization temperatures of the inclusions. The device can operate within a temperature range of -196°C to 600°C, with a heating/freezing rate adjustable from 0.01°C/min to 130°C/min and an accuracy of ±0.1°C.

Determination of homogenization temperatures

The process of determining homogenization temperatures involved a gradual and stable increase in temperature. Initially, the temperature was increased at a rate of 10°C/min. As the temperature approached the phase transition range of the fluid inclusions (between 140°C and 350°C for these analyses), the heating rate was reduced to 1°C/min. After the homogenization of the gas-liquid inclusion, the temperature was cycled around the initial transition point at 5°C/min and then stabilized back to 1°C/min for detailed observation and precise determination of the homogenization temperature.

Determination of freezing point temperature and salinity

The freezing point temperature was determined by cooling the samples. Initially, the temperature was reduced to -30°C at a rate of 20°C/min, followed by heating from

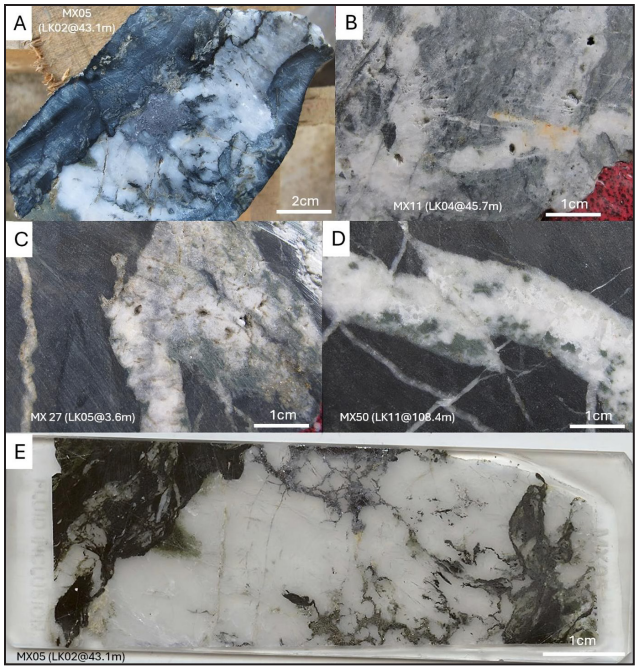

Figure 3: A-D. Representative images of quartz-sulphide hydrothermal veins from the Au-bearing mineralisation zone at the Me Xi deposit, collected for fluid inclusion analyses; E. Representative image of a double-polished thin section prepared from the hand specimen shown in (A).

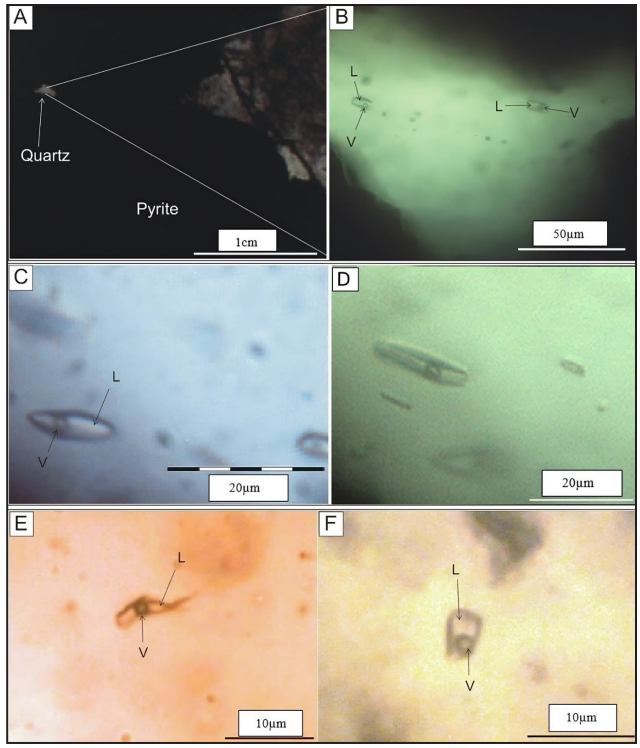

Figure 4: Representative photomicrographs of liquid-rich two-phase fluid inclusions in quartz veins from the Au-bearing stage at the Me Xi gold deposit, central Vietnam: A. Fluid inclusions in quartz trapped inside pyrite, sample No. MX03; B and C. Marked primary fluid inclusions in quartz trapped inside pyrite in (A) D, E and F. Primary fluid inclusions in quartz, sample No. MX05, MX27 and MX44, respectively. Abbreviations: L denotes liquid, V denotes vapour.

-30°C to 5°C at 5°C/min. Close observations were made to identify the complete freezing of the liquid and gas phases, as well as the phase transition point where the solid ice melts entirely (the freezing/melting point, Tm).

The salinity (W) of the solution was calculated based on the Tm value using a equation by Bodnar (1993), which excludes the influence of clathrate compounds (e.g., CO_2, CH_4) since these gases were not detected in the inclusions under the microscope except by Laser Raman Spectroscopy.

$$W=1.78Tm-0.0442Tm^2+0.000557Tm^3$$

Where W is the salinity (in weight percent NaCl), while Tm (°C) is the temperature at which freezing begins, equivalent to the last ice melting temperature after complete freezing of the liquid phase (Tm is taken as the absolute value).

RESULTS

Fluid inclusion petrography

Primary fluid inclusions in the hydrothermal veins from the Au-bearing stage at the Me Xi area are predominantly small (mostly <10 μm) and display various morphologies, ranging from elongated lenticular shapes to nearly spherical forms (Figure 4). In selected samples, only liquid-rich two-phase inclusions were recorded, with the liquid phase typically occupying approximately 70-90% of the inclusion volume (Figure 4). CO_2 is not clearly observed by fluid inclusion petrographic studies.

Late-stage microfractures were frequently observed in the samples, often associated with secondary inclusions. These secondary inclusions are small and exhibit linear or planar distributions, and were not the focus of this study.

Homogenisation temperature and salinity

Results of the thermal analysis of fluid inclusions, including homogenization temperature, last melting point and calculated salinity from Au-bearing stage, are summarized in Table 1 and presented in Figure 5.

The analysis shows that fluid inclusions in quartz have a wide homogenisation temperature range of 181-394°C (n=77), with an average value of ~240°C. Most fluid inclusions crystallised within the lower temperature range of ~180-260°C (n=56), compared to a smaller number that crystallised in the higher temperature range of ~280-350°C (n=18). Only a few inclusions (3 out of 77) have high temperatures of ~380-400°C.

The salinity of the solutions varies widely from ~0.3-16.9 wt.% NaCl (n=57), with an average value of 8 wt.% NaCl. In this group, inclusions with salinity contents greater than 5 wt% account for ~82% of the total population (n= 47) and predominate the dataset.

Table 1: Results of fluid inclusion analyses for quartz from hydrothermal veins of the Au-bearing stage in the Me Xi deposit. Note: FI = fluid inclusion; Th_1, Th_2, Th_3 = first, second and third measurement of homogenisation temperature, respectively; Th_{fn} = averaged homogenisation temperature; Tm_1, Tm_2, Tm_3 = first, second and third measurement of first-melting temperature, respectively; Tm_{fn} = averaged first-melting temperature.

Order	Spl. No.	FI. No.	Homogenisation temperature (°C)				Last melting temperature (°C)				NaCl (wt%)
			Th_1	Th_2	Th_3	Th_{fn}	Tm_1	Tm_2	Tm_3	Tm_{fn}	
1	MX03	1	182.7	182.4		182.6	-0.3	-0.4		-0.35	0.6
2	MX03	3	186.3	186.2		186.3	-2.5	-2.7		-2.60	4.3
3	MX03	5	189.8	189.8		189.8	-2.3	-2.3		-2.30	3.9
4	MX03	6	210	210.6	210.8	210.5	-3.7	-3.3		-3.50	5.7
5	MX03	8	188.7	187.8		188.3	-4.2	-4.0		-4.10	6.6
6	MX03	10	188	188.7		188.4	-4.2	-3.3		-3.75	6.1
7	MX05	1	199.9	200	200.3	200.1	-4.7	-4.7		-4.70	7.4
8	MX05	2	200	200.2	200.5	200.2	-3.2	-3.4		-3.30	5.4
9	MX05	5	183.8	184		183.9					
10	MX05	7	208.8	210.1	209.5	209.5	-5.1	-5.1		-5.10	8.0
11	MX05	8	217.7	219.7	217.7	218.4					
12	MX05	9	205	205.7		205.4	-4.5	-4.4		-4.45	7.1
13	MX05	11	340	340.33		340.2					
14	MX05	12	393	395	393.5	393.8					
15	MX05	13	387	388		387.5					
16	MX05	14	287	288		287.5					
17	MX05	15	215	215		215.0					
18	MX05	16	277	278		277.5					
19	MX11	1	253	252		252.5					
20	MX11	2	211	210.6		210.8	-0.1	-0.2		-0.15	0.3
21	MX11	3	206	205.4		205.7					
22	MX11	4	216	214		215.0	-4.2	-4.6		-4.40	7.0
23	MX11	5	309	311		310.0	-8.7	-8.7		-8.70	12.5
24	MX11	6	315	315		315.0	-8.5	-8.5		-8.50	12.3
25	MX11	7	310	311		310.5	-6.3	-7		-6.65	10.0
26	MX11	8	185	187		186.0	-8.9	-8.5		-8.70	12.5
27	MX11	9	323	323		323.0	-10.6	-10		-10.30	14.3
28	MX11	10	338	338.2		338.1					
29	MX27	6	245	245.6		245.3	-8.7	-9		-8.85	12.7
30	MX27	7	254	254.7		254.4	-8	-7.7		-7.85	11.5
31	MX27	8	203	203.5		203.3					
32	MX27	10	208	209		208.5	-9	-8.7		-8.85	12.7
33	MX27	11	325	326		325.5	-1.3	-1.5		-1.40	2.4
34	MX27	12	188	188.5		188.3					
35	MX27	13	328	329		328.5	-6.5	-6.3		-6.40	9.7
36	MX27	14	228	228.6		228.3					
37	MX27	15	248	248		248.0					
38	MX27	16	256	254.8		255.4	-5.3	-5		-5.15	8.1
39	MX27	2	295	300		297.5	-2.7	-2.8		-2.75	4.6

Table 1: Continued.

Order	Spl. No.	FI. No.	Homogenisation temperature (°C)				Last melting temperature (°C)				NaCl (wt%)
			Th_1	Th_2	Th_3	Th_{fn}	Tm_1	Tm_2	Tm_3	Tm_{fn}	
40	MX27	3	220	220		220.0	-3.4	-3.4		-3.40	5.6
41	MX27	4	190	190.5		190.3	-6.7	-6.4		-6.55	9.9
42	MX27	5	258	257		257.5	-5.4	-5.3		-5.35	8.3
43	MX44	1	215.4	215.6		215.5	-1.3	-1.6		-1.45	2.5
44	MX44	2	339	338.7		338.9	-5.8	-5.6		-5.70	8.8
45	MX44	3	290	290		290.0	-5	-5		-5.00	7.9
46	MX44	4	290	290		290.0	-2.6	-2.8		-2.70	4.5
47	MX44	5	389	390		389.5					
48	MX44	6	310	312		311.0	-4.8	-5		-4.90	7.7
49	MX44	7	206	206.2		206.1	-5.5	-5.5		-5.50	8.5
50	MX44	8	194	194		194.0	-13	-13.1		-13.05	16.9
51	MX44	11	182	182		182.0	-6.5	-6		-6.25	9.5
52	MX44	13	213	214		213.5	-10	-8.3		-9.15	13.0
53	MX44	14	227.9	227.5		227.7	-11.5	-11.5		-11.50	15.5
54	MX44	15	347.8	347.8		347.8					
55	MX44	16	260	260		260.0	-6	-6		-6.00	9.2
56	MX44	17	199	199		199.0	-1	-1		-1.00	1.7
57	MX44	18	330	330		330.0					
58	MX44	19	308.7	308.6		308.7					
59	MX31	1	187	187		187.0	-3.3	-3.3		-3.30	5.4
60	MX31	2	187.7	187.7		187.7	-2	-1.4		-1.70	2.9
61	MX31	4	182	182.2		182.1	-3.4	-3.4		-3.40	5.6
62	MX31	5	190	190.4		190.2	-3.2	-3.3		-3.25	5.3
63	MX31	6	181	181		181.0	-4	-4		-4.00	6.4
64	MX31	7	186.9	187		187.0	-3.6	-3.5		-3.55	5.8
65	MX31	8	192.8	193		192.9	-3.6	-3.5		-3.55	5.8
66	MX31	9	225	225.5		225.3	-3.4	-3.6		-3.50	5.7
67	MX31	10	205	205		205.0	-3	-3		-3.00	5.0
68	MX50	1	198	200		199.0	-7	-7		-7.00	10.5
69	MX50	2	218	218		218.0	-7.6	-7.9		-7.75	11.4
70	MX50	3	206	206		206.0	-5	-5.4		-5.20	8.1
71	MX50	4	203	202.2		202.6	-5	-5		-5.00	7.9
72	MX50	5	207	207		207.0	-7.5	-7.5		-7.50	11.1
73	MX50	6	209	209.2		209.1	-8	-8.2		-8.10	11.8
74	MX50	7	189	190		189.5	-9	-8.7		-8.85	12.7
75	MX50	8	207	207		207.0					
76	MX50	9	206	205.8		205.9	-5.6	-5.4		-5.50	8.5
77	MX50	10	193	192		192.5	-6	-6		-6.00	9.2

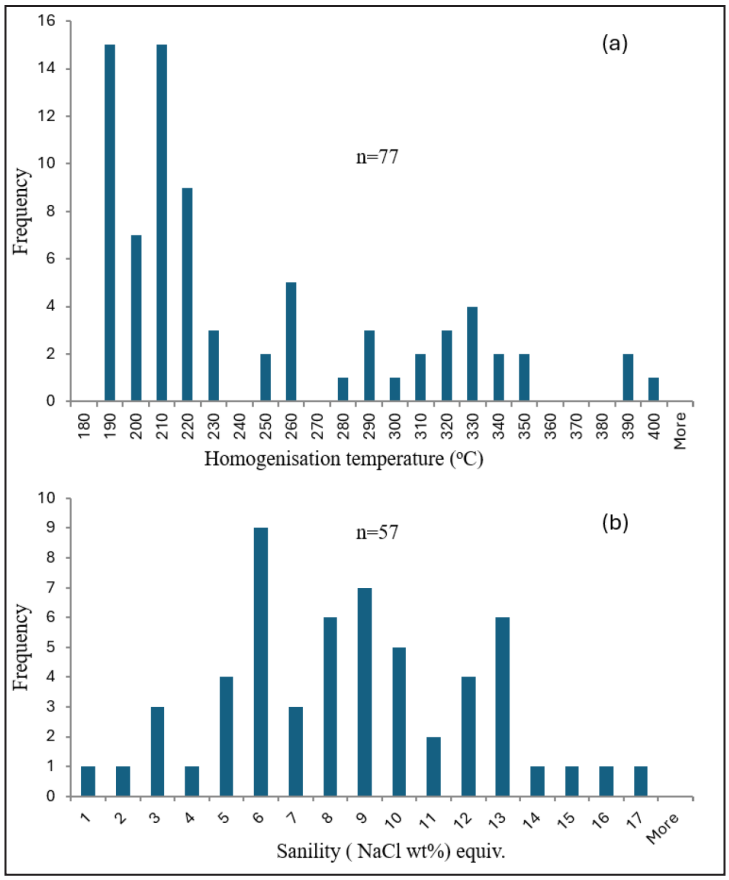

Figure 5: Analysis results for fluid inclusion from quartz in the Au-bearing stage: (a) Plot of homogenisation temperatures versus salinities (n=77, min = 181°C, max = 394°C, average = 240°C; (b) Frequency distribution chart of salinities (n=57, min = 0.3 wt% NaCl, max = 16.9 wt% NaCl, average = 8 wt.% NaCl).

DISCUSSION

Source(s) of fluids

The salinity value is an important indication for the sources of fluids in a hydrothermal system (Wilkinson, 2001; Bodnar *et al*., 2014). In general, fluids sourced from magmatic system, such as porphyry and skarn deposits, have moderate to high salinity values (commonly > 5%) whereas those from non-evaporite sedimentary sequences, sea water, or meteoric water have low salinity values (commonly <5%; Bodnar *et al*., 2014).

Fluid inclusions in quartz from the hydrothermal Au-bearing stages at the Me Xi deposit exhibit a wide range of salinity, from 0.3 to 17 wt. % NaCl, with an average of ~8 wt.% NaCl. The salinity values of ore-bearing fluids are predominantly greater than 5 wt% (ie., ~5-17. wt.%), accounting for ~82% of the population (n=47/57), indicates a significant magmatic contribution (Bodnar, 1993; Bodnar *et al*., 2014). The sulphur isotopic study results (mainly from -4.6 ‰ to -2.5 ‰) at the Me Xi from Le *et al*. (2025) further support a predominantly magmatic fluid source.

In the geological context of the Me Xi area where the mineralisation is about 3km from the ~430 Ma dolerite (Le *et al*., 2026), the magmatic-sourced fluids are most likely linked to this type of magma. On a regional scale, the magmatic history in the TSB encompasses two main stages: O-S Caledonian and the P-T_1 Indosinian orogenies. The Caledonian mineralising events have been documented within the TSB, with Donken Cu-Au deposits in southern Laos (Gardner *et al*., 2017) and the Duc Bo Au-Pb-Zn deposit in central Vietnam (Khin Zaw *et al*., 2014). Regarding the late tectonic event, to date, no magmatic occurrence has been recorded at the Me Xi Au area, but regional magmatism is evident. About ~45 km to west of Me Xi, ~280-300 Ma rhyodacite porphyry associated with Cu-Au mineralisation at the Sepon Mineral District, Laos have been well defined (Cromie, 2010). To the southern end of TSB, in the TPSZ, ~ 270-220 Ma igneous rocks and related Au mineralisation (~250-220 Ma; Manaka, 2014) at the Phuoc Son Au deposits and ~ 240 Ma leucocratic dyke and coeval skarn type Au-W system at Bong Mieu deposits (Khin Zaw *et al*., 2014) have been identified. Thus, a hidden P-T_1 magmatic event at depth may have contributed to the late mineralising event at Me Xi.

In contrast, a minor population (~18%, n = 10/57) of low-salinity fluids (~0.3–5 wt.% NaCl equiv.), in comparison

with the results from Roedder (1984) and Bodnar *et al*. (2014), these fluids could be derived from (1) the infiltration of meteoric water, (2) water-rock interaction at shallower crustal levels, (3) seawater, and/or (4) metamorphic water. The lack of metamorphic-derived gases such as CO_2 and CH_4 is generally suggests a limited contribution from metamorphic fluids although the sedimentary rocks that host gold mineralisation in this deposit, as well as in similar deposits nearby, have undergone metamorphism at greenschist to amphibolite facies (Wilkinson, 2001; Bodnar *et al*., 2014). The moderate to high salinity coupled with relatively low homogenization temperatures observed in the fluid inclusions are inconsistent with a significant metamorphic fluid contribution, which typically exhibits higher homogenization temperatures and lower salinities (generally <7 wt.% NaCl equiv.) (Wilkinson, 2001; Bodnar *et al*., 2014). Moreover, there is no direct evidence presented in the region to suggest a direct seawater source during the mineralization event at Me Xi.

Given the data set and the geological and metallogenic context of the Truong Son Belt, the fluid inclusion study results indicate that the ore-forming fluids at Me Xi were primarily magmatic in origin, with minor dilution or modification by meteoric waters and/ or water-rock interaction at shallower crustal levels, while metamorphic fluids played a negligible role in the mineralizing system.

Temperature of the ore formation

The homogenization temperatures (Th) for fluid inclusions from the Au-bearing stage at the Me Xi deposit range from 181-394°C, with most inclusions homogenizing between 180-260°C. This dataset provides insights into the mineralisation styles and the physical condition of mineralisation. The low-temperature range (180-260°C), which dominates the population (n=56), indicate that the hydrothermal fluids and metals at the Me Xi area were mainly accumulated at low temperatures (i.e., 180-260°C), which is consistent with the dominant stockwork textures recorded in the mineralisation zones. This dominantly low Th range at the Me Xi area suggests that the mineralisation occurred at shallow crustal levels, with the potential for deeper zones where mineralisation likely formed under higher temperature conditions. The small number of inclusions with moderate (280-350°C, n=18) and high (380-400°C, n=3) temperature ranges suggest a potential of deeper-seated hydrothermal activity and/or magmatic input.

Ore precipitation

Shepherd *et al*. (1985) proposed a plot for dynamic hydrothermal systems based on homogenisation temperature against salinity for fluid inclusions to constrain the fluid processes, such as fluid mixing, boiling, cooling and dilution. In comparison to the model for fluid evolution of Shepherd *et al*. (1985), the homogenisation temperature and salinity values at the Me Xi area are consistent with

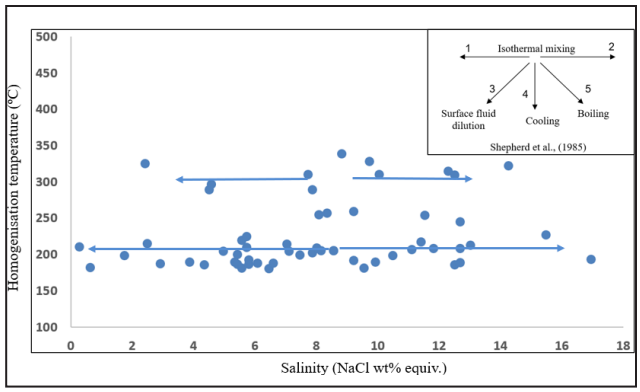

Figure 6: Plot of homogenisation temperatures against salinities for primary fluid inclusions from Au-bearing hydrothermal stages at the Me Xi deposit, central Vietnam compared to the model of fluid processes defined by Shepherd *et al*. (1985) as shown in the inset figure.

an isothermal mixing trend between high and low salinity fluids (Figure 6). This mixing process possibly occurred between magmatic-sourced fluids and meteoric fluids or water-rock interaction involving the carbonaceous sedimentary host rocks respectively, as being discussed above. The suggested magmatic fluid is supported by the coeval timing of mineralisation and intrusive event at the Me Xi area (Le *et al*., 2026).

The studied results provide new insights into fluid evolution, temperature regimes and sources of ore-bearing fluids at the Me Xi Au deposit in central Truong Son Belt. The findings not only provide a valuable fluid inclusion dataset and corresponding interpretations for mineralisation at the Me Xi but also confirm the role of magmatic contributions in Au metallogeny in the central Truong Son Belt. This contributes to the regional Au metallogenic models and helps guide future exploration strategies.

CONCLUSIONS

The fluid inclusion studies from the Me Xi Au deposit in the central TSB provide critical insights into the physico-chemical conditions and origin of Au mineralisation. The primary fluid inclusions in selected samples are predominantly small (mostly <10 μm), consisting exclusively of two-phase (liquid and vapor) inclusions, with liquid occupying approximately of 70-90% of volumes. The studied results reveal a wide range of homogenisation temperatures (181-394°C), with the majority of low temperatures (180-260°C, n=56), which correlates well with the stockwork textures observed. A smaller population of inclusions formed at higher temperatures (280-394°C, n=21), suggesting deeper-seated hydrothermal and/or magmatic input. Fluid salinities also exhibit a broad range (0.3-16.9 wt.% NaCl), with an average of ~8 wt.% NaCl, indicating a mixed origin of hydrothermal fluids. Low-salinity fluids (~0.3-5 wt.% NaCl) are likely linked to meteoric water or diluted hydrothermal fluids, whereas moderate- to high-salinity inclusions (~5-17 wt.% NaCl) suggest a significant magmatic

contribution, potentially sourced from the nearby ~430 Ma dolerite and/or hidden Permian-Triassic magmatic activities.

The fluid inclusion data support an isothermal mixing model involving low-salinity fluids and high-salinity magmatic fluids. This mixing process likely occurred in a shallow-crustal environment, consistent with the stockwork vein observed at Me Xi.

The study results provide the first comprehensive fluid inclusion evidence for magmatic and meteoric fluid mixing or water-rock interaction at the Me Xi deposit, and highlight the importance of fluid evolution in gold mineralisation systems in central Vietnam. The study significantly contributes to the metallogenic framework of the central Truong Son Belt and may guide future exploration models for similar deposits in the region.

ACKNOWLEDGEMENT

We would like to express our gratitude to the study project on Au metallogeny in the central Truong Son Belt (code B2024-MDA-04) for its support. Special thanks go to Dr. Abhisit Salam, Mr. Le Van Hai, Mr. Nguyen Van Dai and other personnel from the Southeast Asia Ore Deposit Research Project at CODES, University of Tasmania, for their invaluable assistance in studying the Me Xi Au deposit. We extend our sincere thanks to the peer reviewers and the editorial board for their constructive feedback, which significantly improved the quality of this manuscript. We also gratefully acknowledge the CODES Centre of Ore Deposit and Earth Sciences, University of Tasmania, for providing the analytical facilities that made this study possible.

AUTHORS CONTRIBUTION

TXL is the main author who prepared the manuscript and figures, analysed and compiled data. KZ, HTT, KQL, DKN, BXT provided support on the regional studies and deposit mapping. All authors reviewed the results, interpretation and edited the manuscript.

CONFLICT OF INTEREST

No potential conflict of interest was reported by the authors.

REFERENCES

Axiom, 2006. Axiom Mining LTD Prospectus, Company Report.

Bodnar, R., 1993. Revised equation and table for determining the freezing point depression of H_2O-NaCl solutions. Geochimica et Cosmochimica acta, 57, 683-684.

Bodnar, R., Lecumberri-Sanchez, P., Moncada, D., & Steele-MacInnis, M., 2014. Fluid inclusions in hydrothermal ore deposits. In: Karl K. Turekian, & Heinrich D. Holland (Eds.), Treatise on geochemistry vol. 13. Elsevier Ltd, Oxford. 649 p. https://doi.org/10.1016/B978-0-08-095975-7.01105-0.

Carter, A., Roques, D., Bristow, C., & Kinny, P., 2001. Understanding Mesozoic accretion in Southeast Asia: Significance of Triassic thermotectonism (Indosinian orogeny) in Vietnam. Geology, 29, 211-214.

Cromie, P.W., 2010. Geological setting, geochemistry and genesis of the Sepon gold and copper deposits, Laos. Ph.D Thesis, University of Tasmania.

Dung, N.T., Anh, T.T., Hieu, P.T., Minh, P., Truong, L.X., Minh, N.T., & Hung, D.D., 2024. Crustal evolution of Paleozoic-Mesozoic granitoid in Dakrong-A Luoi area, Truong Son belt, central Vietnam: evidence from zircon U-Pb geochronology, geochemistry, and Hf isotope composition. International Geology Review, 66(17), 1-25. https://doi.org/10.1080/00206814.2024.2315554.

Duong, N.X., Ngat, D.H., Chi, D.V., Thuoc, H.V., Kinh, H.D., Lan, L., & Thuan, P.V., 1996. Geological Map Le Thuy - Quang Binh, Scale 1:200 000.

Gardner, C.J., Graham, I.T., Belousova, E., Booth, G.W., & Greig, A., 2017. Evidence for Ordovician subduction-related magmatism in the Truong Son terrane, SE Laos: Implications for Gondwana evolution and porphyry Cu exploration potential in SE Asia. Gondwana Research, 44, 139-156.

Hieu, P.T., Chen, F.K., Thuy, N.T.B., Cường, N.Q., & Li, S.Q., 2013. Geochemistry and zircon U-Pb ages and Hf isotopic composition of Permian alkali granitoids of the Phan Si Pan zone in northwestern Vietnam. Journal of Geodynamics, 69, 106-121.

Hieu, P.T., Li, S.Q., Yu, Y., Thanh, N.X., Dung, L.T., Tu, V.L., Siebel, W., & Chen, F., 2017. Stages of late Paleozoic to early Mesozoic magmatism in the Song Ma belt, NW Vietnam: evidence from zircon U-Pb geochronology and Hf isotope composition. International Journal of Earth Sciences, 106, 855-874.

Hieu, P.T., Yang, Y.Z., Binh, D.Q., Nguyen, T.B.T., Dung, L.T., & Chen, F., 2015. Late Permian to Early Triassic crustal evolution of the Kontum massif, central Vietnam: zircon U–Pb ages and geochemical and Nd–Hf isotopic composition of the Hai Van granitoid complex. International Geology Review, 57, 1877-1888.

Hoa, T.T., Anh, T.T., Phuong, N.T., Dung, P.T., Anh, T.V., Izokh, A.E., Borisenko, A.S., Lan, C., Chung, S., & Lo, C., 2008. Permo-Triassic intermediate–felsic magmatism of the Truong Son belt, eastern margin of Indochina. Comptes Rendus Geoscience, 340, 112-126.

Hung, D.D., Tsutsumi, Y., Hieu, P.T., Minh, N.T., Minh, P., Dung, N.T., Hung, N.B., Komatsu, T., Hoang, N., & Kawaguchi, K., 2022. Van Canh Triassic granite in the Kontum Massif, central Vietnam: geochemistry, geochronology, and tectonic implications. Journal of Asian Earth Sciences X, 7, 100075. https://doi.org/10.1016/j.jaesx.2021.100075.

Jiang, W., Yu, J.H., Wang, X., Griffin, W., Pham, T., Nguyen, D., & Wang, F., 2020. Early Paleozoic magmatism in northern Kontum Massif, Central Vietnam: Insights into tectonic evolution of the eastern Indochina Block. Lithos, 376, 105750. https://doi.org/10.1016/j.lithos.2020.105750.

Khin Zaw, Meffre, S., Lai, C.-K., Burrett, C., Santosh, M., Graham, I., Manaka, T., Salam, A., Kamvong, T., & Cromie, P., 2014. Tectonics and metallogeny of mainland Southeast Asia - A review and contribution. Gondwana Research, 26(1), 5-30. https://doi.org/10.1016/j.gr.2013.10.010.

Lepvrier, C., Maluski, H., Tich, V., Leyreloup, A., Thi, P.T., & Vuong, N., 2004. The Early Triassic Indosinian orogeny in Vietnam (Truong Son Belt and Kontum Massif); implications for the geodynamic evolution of Indochina. Techtonophysics, 393, 87-118.

Le, T.X., H.T. Tran, L.Q. Nguyen, Z. Khin, & S. Abhisit. 2015. Gold fineness and pyrite geochemistry: Evidences for physico-

chemical conditions and genesis of ore-bearing fluids at Me Xi Au Deposit, Quang Tri, Vietnam. Journal of Mining and Earth Sciences, 4, 8.

Le, T.X., Tran, H.T., Zaw, K., & Le, T.T., 2024. Geological setting and gold mineralisation characteristics at the Me Xi, Vinh Linh, Quang Tri, Vietnam. Journal of Mining and Earth Sciences, 65(6), 58-69. https://doi.org/10.46326/JMES.2024.65(6).06.

Le, T.X., Zaw, K., & To, B.X., 2025. Sources of Au-bearing mineralisation at the Me Xi Au deposit, Central Truong Son Belt, Vietnam: Evidence from sulfur isotopic composition. Journal of Mining and Earth Sciences, 66(3), 29-38. (in Vietnamese).

Le, T.X., Zaw, K., Tran, H.T., Meffre, S., Hieu, P.T., Khang, L.Q., Luyen, N.D., & Tuong, D.T., 2026. Early Paleozoic magmatism and Au mineralisation in the Central Truong Son Belt: Insights from geochronology and lead isotope at the Me Xi gold deposit. J. Asian Earth Sci., 298, 106938.

Liu, J., Tran, M.D., Tang, Y., Nguyen, Q. L., Tran, T.H., Wu, W., Chen, J., Zhang, Z., & Zhao, Z., 2012. Permo-Triassic granitoids in the northern part of the Truong Son belt, NW Vietnam: Geochronology, geochemistry and tectonic implications. Gondwana Research, 22, 628-644.

Maluski, H., Lepvrier, C., Leyreloup, A., Tich, V.V., & Thi, P.T., 2005. 40Ar–39Ar geochronology of the charnockites and granulites of the Kan Nack complex, Kon Tum Massif: Vietnam. Journal of Asian Earth Sciences, 25, 653-677.

Manaka, T., 2008. Geological Setting and Mineralisation Characteristics of The Long Chieng Track and Ban Houayxai Deposit, Lao PDR. Master Thesis, University of Tasmania.

Manaka, T., 2014. A study of mineralogical, geochemical and geochronological characteristics and ore genesis in Phuoc Son Gold deposit area, Central Vietnam. Unpub. PhD thesis, University of Tasmania.

Minh, N.T., Dung, N.T., Hung, D.D., Minh, P., Yu, Y., & Hieu, P.T., 2020. Zircon U-Pb ages, geochemistry and isotopic characteristics of the Chu Lai granitic pluton in the Kontum massif, central Vietnam. Mineralogy and Petrology, 114, 289-303.

Minh, P., Hieu, P.T., & Hoang, N.K., 2018. Geochemical and geochronological studies of the Muong Hum alkaline granitic pluton from the Phan Si Pan Zone, northwest Vietnam: Implications for petrogenesis and tectonic setting. Island Arc, 27(4), e12250. https://doi.org/10.1111/iar.12250.

Nagy, E.A., Maluski, H., Lepvrier, C., Schärer, U., Thi, P.T., Leyreloup, A., & Thich, V.V., 2001. Geodynamic significance of the Kontum massif in central Vietnam: composite 40Ar/39Ar and U-Pb ages from Paleozoic to Triassic. The Journal of Geology, 109, 755-770.

Roedder, E., 1984. Reviews in Mineralogy Volume 12: Fluid Inclusions. Mineralogical Society of America, Virginia, USA. 644 p.

Roger, F., Jolivet, M., Maluski, H., Respaut, J.P., Münch, P., Paquette, J.L., Vu Van, T., & Nguyen Van, V., 2014. Emplacement and cooling of the Dien Bien Phu granitic complex: Implications for the tectonic evolution of the Dien Bien Phu Fault (Truong Son Belt: NW Vietnam). Gondwana Research, 26, 785-801.

Roger, F., Leloup, P.H., Jolivet, M., Lacassin, R., Trinh, P.T., Brunel, M., & Seward, D., 2000. Long and complex thermal history of the Song Chay metamorphic dome (Northern Vietnam) by multi-system geochronology. Tectonophysics, 321, 449-466.

Shepherd, T., Rankin, A.H., & Alderton, D.H.M., 1985. A practical guide to fluid inclusion studies. Blackie, Glasgow. 235 p.

Shi, M.F., Lin, F.C., Fan, W.Y., Deng, Q., Cong, F., Tran, M.D., Zhu, H.P., & Wang, H., 2015. Zircon U–Pb ages and geochemistry of granitoids in the Truong Son terrane, Vietnam: Tectonic and metallogenic implications. Journal of Asian Earth Sciences, 101, 101-120.

Thanh, T.V., Hieu, P.T., Minh, P., Nhuan, D.V., & Thuy, N.T.B., 2019. Late Permian-Triassic granitic rocks of Vietnam: the Muong Lat example. International Geology Review, 61, 1823-1841.

Thuy, N.T.B., Xuan, N.T., Anh, B.t., Minh, P., Hieu, P.T., & Binh, D.Q., 2024. Early Paleozoic tectonic evolution in the central Vietnam: evidence from geochronological and geochemical constraints. International Geology Review, 1-17. https://doi.org/10.1080/00206814.2024.2366972.

Tran, H.T., Zaw, K., Halpin, J.A., Manaka, T., Meffre, S., Lai, C.K., Lee, Y., Le, H.V., & Dinh, S., 2014. The Tam Ky-Phuoc Son Shear Zone in central Vietnam: Tectonic and metallogenic implications. Gondwana Research, 26, 144-164.

Tran Van Tri, Vu Khuc, Bui Minh Tam, Cu Minh Hoang, Dang Tran Huyen, Doan Nhat Truong, Le Do Binh, Nguyen Xuan Bao, Tong Duy Thanh, Tran Ngoc Nam, Tran Thanh Hai, Tran Tuan Anh, Tran Trong Hoa, & Tran Ngoc Nam, 2009. Geology and natural resources of Vietnam. Natural Sciences and Technology Publishing House, Hanoi. 589 p. (in Vietnamese).

Trong, N.H., Zong, K., Liu, Y., Yuan, Y., Hieu, P.T., Dung, L.T., & Minh, P., 2021. Early Paleozoic Arc Magmatism and Accretionary Orogenesis in the Indochina Block, Southeast Asia. The Journal of Geology, 129, 33-48.

Wang, S., Mo, Y., Wang, C., & Ye, P., 2016. Paleotethyan evolution of the Indochina Block as deduced from granites in northern Laos. Gondwana Research, 38, 183-196.

Wilkinson, J.J., 2001. Fluid inclusions in hydrothermal ore deposits. Lithos, 55, 229-272.

Żelaźniewicz, A., Hòa, T.T., & Larionov, A.N., 2013. The significance of geological and zircon age data derived from the wall rocks of the Ailao Shan–Red River Shear Zone: NW Vietnam. Journal of Geodynamics, 69, 122-139.

Zhang, R.Y., Lo, C.H., Chung, S.L., Grove, M., Omori, S., Iizuka, Y., Liou, J.G., & Tri, T.V., 2013. Origin and Tectonic Implication of Ophiolite and Eclogite in the Song Ma Suture Zone between the South China and Indochina Blocks. Journal of Metamorphic Geology, 31, 49-62.

Manuscript received 15 March 2025;
Received in revised form 31 May 2025;
Accepted 15 July 2025
Available online 29 May 2026